



BULLKID: BULky and Low-Threshold Kinetic Inductance Detectors

I. Colantoni^{1,2}  · C. Bellenghi² · M. Calvo³ · R. Camattari⁴ · L. Cardani² · N. Casali² · A. Cruciani² · S. Di Domizio⁵ · J. Goupy³ · V. Guidi^{4,6} · H. Le Sueur⁷ · M. Martinez⁸ · A. Mazzolari⁴ · A. Monfardini³ · V. Pettinacci² · G. Pettinari⁹ · M. Romagnoni^{4,6} · M. Vignati²

Received: 5 August 2019 / Accepted: 10 February 2020 / Published online: 24 February 2020
© Springer Science+Business Media, LLC, part of Springer Nature 2020

Abstract

BULLKID is an R&D project on a cryogenic particle detector to search for rare low-energy processes such as low-mass dark matter and neutrino coherent scattering off nuclei. The detector unit we are designing consists in an array of ~100 silicon absorbers sensed by phonon-mediated, microwave-multiplexed kinetic inductance detectors, with energy threshold below 100 eV and total target mass around 30 g. The single detector unit will be engineered to ensure a straightforward scalability to a future kg-scale experiment.

Keywords Dark matter · Kinetic inductance detectors · Coherent scattering

✉ I. Colantoni
ivan.colantoni@cnr.it

¹ Consiglio Nazionale delle Ricerche, Istituto di Nanotecnologia (CNR - NANOTEC), c/o Dip. Fisica, Sapienza Università di Roma, 00185 Rome, Italy

² INFN - Sezione di Roma, 00185 Rome, Italy

³ Institut Neel, CNRS, Université Grenoble Alpes, 25 Avenue des Martyrs, 38042 Grenoble, France

⁴ INFN - Sezione di Ferrara, 44122 Ferrara, Italy

⁵ Dipartimento di Fisica, Università di Genova, 16146 Genoa, Italy

⁶ Dipartimento di Fisica e Scienze della Terra, Università degli Studi di Ferrara, 44122 Ferrara, Italy

⁷ CEA-Saclay, 91191 Gif-Sur-Yvette Cedex, France

⁸ Laboratorio de Física Nuclear y Astropartículas, Universidad de Zaragoza, C/Pedro Cerbuna 12, 50009 Zaragoza, Spain

⁹ Consiglio Nazionale delle Ricerche, Istituto di Fotonica e Nanotecnologie (CNR - IFN), Via Cineto Romano 42, 00156 Rome, Italy

1 Introduction

WIMPs (weakly interacting massive particles) are ideal candidates as dark matter particles [1], and the majority of experiments are currently focused on its discovery by implementing the direct detection of the elastic scattering off nuclei. A tremendous increase in the target mass of the detectors in the last 10 years boosted the sensitivity by several orders of magnitude, but dark matter particles are still undetected. Alternative models are being proposed, most of them pointing to particles with mass smaller than $1 \text{ GeV}/c^2$, such as the SIMPs (strongly interacting massive particles). The detection of SIMPs and other light particles requires sensors with small energy threshold, and total target mass greater than 100 g. A first limit, based on a 0.5 g cryogenic detector, has been published recently [2, 3], with large room of improvement for a more massive target.

The discovery of the coherent elastic neutrino-nucleus scattering in 2017 by the COHERENT collaboration [4] opened new opportunities to search for new physics (e.g., flavor changing neutral currents) via precision measurement of the cross section at different neutrino energies. These measurements could also provide information about the solar neutrino background for dark matter searches and about the neutron form factor, a key ingredient to understand the physics of supernovae explosions [5]. Several new experiments are being proposed, CONNIE [6], CONUS [7], Ricochet at Chooz [8], NUCLEUS [3] and others aiming at the detection of reactor neutrinos. However, with sufficiently sensitive and scalable detectors, the precision would be larger, and low-energy neutrinos produced by radioactive sources like ^{51}Cr could be studied.

BULLKID is an R&D for new experiments on sub-GeV dark matter and coherent neutrino-nucleus scattering which leverages the sensitivity and high multiplexing capability of superconducting microwave kinetic inductance detectors (MKIDs) [9] to reach low energy thresholds and high target masses. The detector is based on the technology of phonon-mediated MKIDs [10] and further developed with CALDER [11]: Particles interact with a silicon substrate and generate athermal phonons that scatter through the substrate until they are absorbed and generate a signal in Al [12] or Al–Ti–Al [13] MKIDs deposited on the surface. The dark matter or neutrino target of BULLKID will consist in a $5 \times 5 \times 5 \text{ mm}^3$ silicon voxel (Fig. 1, left). To exploit the MKID multiplexing several voxels will be carved from a single 5-mm-thick 3" silicon wafer: One side of the wafer will host the lithography, with a single feedline running through all the MKIDs; the opposite side will be cut into a square grid of 5 mm pitch with a 4.5 mm dice depth, so as to obtain almost cubic voxels, and leave the surface hosting the MKIDs intact (Fig. 1, center and right). In this way, the phonons produced in a voxel will be isolated and absorbed by a single MKID to improve the signal-to-noise ratio. This geometry also ensures an efficient background reduction, as multiple-voxel events can only be generated by cosmic rays or natural radioactivity and not by neutrinos or dark matter particles. Around 100 voxels of 0.29 g each can be obtained from a 5-mm-thick 3" wafer, for a total active detector mass of 29 g. In a future experiment several wafer would be stacked to reach higher target masses.

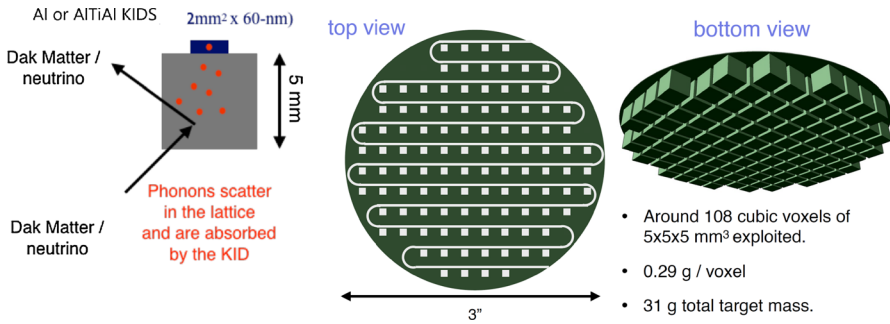


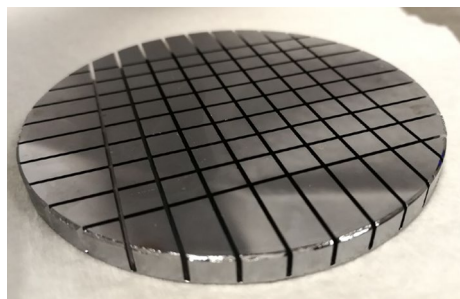
Fig. 1 Left: One BULLKID $5 \times 5 \times 5 \text{ mm}^3$ voxel, where impinging particles produce athermal phonons that convert into a signal in the MKID deposited on a surface. Right: Array of voxels carved from a single 3" silicon wafer 5-mm-thick with the patterned MKIDs. (Color figure online)

The best energy resolution achieved by CALDER is $25 \text{ eV } \sigma$ [13], while in BULLKID a 5σ energy threshold below 100 eV is needed, possibly down to 20 eV. On one side, the phonon collection is expected to be larger, as in CALDER part of the phonons is absorbed by the feedline which is 2 cm long, while in BULLKID the feedline on top of a single voxel is restricted to 5 mm; on the other side while in CALDER a significant part of the phonons is absorbed by the wafer supports, in BULLKID the voxel support structure is absent, being the array a monolithic silicon structure. The voxel size will be optimized in the future to obtain the best compromise between sensitivity and total number of resonators. In the following, we report on the first steps of the project: the results from the wafer dicing and the description of a prototype KID.

2 Fabrication

Voxels are diced from a 5-mm-thick 3" silicon wafer using a “Disco DAD 3220” dicer, with fine-grit blade to minimize the mechanical damage during the cut (Fig. 2). The diamond blade having an average grains size of $1 \mu\text{m}$ and thickness $500 \mu\text{m}$ can rotate at 30,000 rpm (JP1E5746 disco.co.jp). The wafer to be diced is mount on a vacuum chuck. The cutting process induces large mosaicity to the

Fig. 2 Test wafer diced to create the cubic voxels. Each voxel is $5 \times 5 \text{ mm}^2$ and 4.5 mm height. The thickness of the un-machined wafer is around 0.5 mm and could be further reduced to reduce the phonon cross talk between voxels. The KID lithography will be made on the side opposite to the machined one. (Color figure online)



surface exposed to the diamond saw, with the formation of a region of $\sim 10 \mu\text{m}$ of amorphous silicon [14]. This damaged region acts as a possible trap for the phonons, so it will be etched in HNA solution 2:15:15 ($\text{HF}:\text{HNO}_3:\text{CH}_3\text{COOH}$). Such etching mixture is widely used in silicon micromachining [15].

The fabrication of the chip will be made using standard photolithography and wet etch approach. After the lithography, the 5-mm-thick wafer is dipped for 60 s in dilute 5% HF solution and then rinsed in deionized water for 60 s and nitrogen dried. The wafer is then moved to an electron beam evaporator dedicated to superconducting materials, where the layers Al–Ti–Al (13–33–30 nm) are subsequently evaporated at rates of 0.5 nm/s in a residual vacuum of 4×10^{-8} mbar. This is important especially for Ti to avoid trapping impurities in the layer [16].

3 Design

The BULLKID prototype single pixel is shown in Fig. 3 and consists of an inductive meander with connected strips, being the active area of the detector, and a capacitor with interdigitated fingers. The capacitance is chosen to keep the current flowing through the meander uniform. Uniform current distribution in meandered zone implies that the shift in resonant frequency due to cooper pair breaking will be the same in the whole area. The pixel is inductively coupled to a Nb coplanar waveguide and ground plane.

We are developing four different geometries in order to optimize the total phonon absorption efficiency of our detector. The CALDER-like prototype A is shown in Fig. 3a, and the total active area of the detector is $2.84 \text{ mm} \times 2.84 \text{ mm}$ and

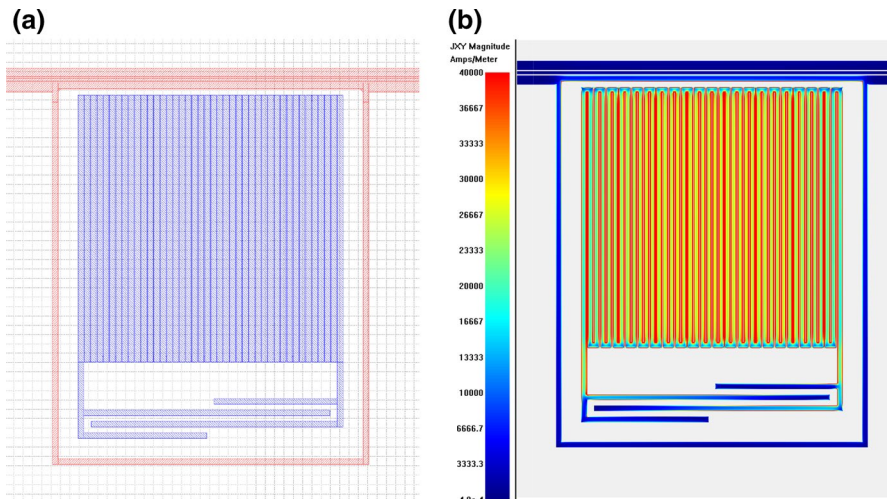


Fig. 3 CALDER-like prototype A. **a** The pixel (violet) is composed of an inductive meander, which is the active area, and an interdigitated capacitor to control the resonant frequency and to make the current across the inductor uniform. **b** The current distribution at the resonant frequency for the prototype A (5×10^{-4} A/m in blue, 40,000 A/m in red). (Color figure online)

consists of an inductive meander with connected strips of $60\ \mu\text{m} \times 2.84\ \text{mm}$. The total active area of all the other is slightly different, while the inductive meander is, respectively, $60\ \mu\text{m} \times 3.40\ \text{mm}$ (prototype B), $28\ \mu\text{m} \times 3.10\ \text{mm}$ (prototype C) and $20\ \mu\text{m} \times 3.00\ \text{mm}$ (prototype D).

Acknowledgements The authors thank the personnel of INFN Sezione di Roma for the technical support, M. Iannone and A. Girardi.

References

1. G. Bertone, D. Hooper, J. Silk, *Phys. Rep.* **405**, 279 (2005). <https://doi.org/10.1017/CBO9780511770739>
2. J.H. Davis, *Phys. Rev. Lett.* **119**, 211302 (2017). <https://doi.org/10.1103/PhysRevLett.119.211302>
3. R. Strauss et al., *Eur. Phys. J. C* **77**, 506 (2017). <https://doi.org/10.1140/epjc/s10052-017-5068-2>
4. US Cosmic Visions: New Ideas in Dark Matter 2017. [arXiv:1707.04591](https://arxiv.org/abs/1707.04591)
5. COHERENT Collaboration, *Science* **357**, 1123 (2017). <https://doi.org/10.1126/science.aao0990>
6. J. Billard, J. Johnston, B.J. Kavanagh, [arXiv:1805.01798](https://arxiv.org/abs/1805.01798)
7. CONNIE Collaboration, *J. Phys. Conf. Ser.* **761**, 012057 (2016). <https://doi.org/10.1088/1742-6596/761/1/012057>
8. M. Lindner, W. Rodejohann, X. Xu, *JHEP* **1703**, 097 (2017). [https://doi.org/10.1007/JHEP03\(2017\)097](https://doi.org/10.1007/JHEP03(2017)097)
9. Day et al., *Nature* **425**, 817 (2003). <https://doi.org/10.1038/nature02037>
10. D.C. Moore et al., *J. Low Temp. Phys.* **167**, 329 (2012). <https://doi.org/10.1007/s10909-011-0434-1>
11. E.S. Battistelli et al., CALDER. *EPJ C* **75**, 353 (2015). <https://doi.org/10.1140/epjc/s10052-015-3575-6>
12. L. Cardani et al., CALDER. *Appl. Phys. Lett.* **110**, 033504 (2017). <https://doi.org/10.1063/1.4974082>
13. L. Cardani et al., CALDER. *SUST* **31**, 075002 (2018). <https://doi.org/10.1088/1361-6668/aac1d4>
14. S. Baricordi et al., *Appl. Phys. Lett.* **91**, 061908 (2007). <https://doi.org/10.1063/1.2768200>
15. K.R. Williams et al., *J. Microelectromech. Syst.* **12**(6), 1057-7157/03 (2003)
16. A. Peruzzi, E. Gottardi, I. Peroni, G. Ponti, G. Ventura, *Nucl. Phys. B* **78**, 576 (1999). [https://doi.org/10.1016/S0920-5632\(99\)00607-6](https://doi.org/10.1016/S0920-5632(99)00607-6)

Publisher's Note Springer Nature remains neutral with regard to jurisdictional claims in published maps and institutional affiliations.